TECHNISCHE MECHANIK 10(1989) Heft 1
Manuskripteingang: 30. 09. 1988

Microstructural Fracture Criteria in Engineering Alloys

J. F. Knott

Introduction

The type of fracture of most concern to an engineer is one which occurs at a stress below design stress, i. e. the general yield stress, divided by a safety factor. Such fracture would be described as „brittle", regardless of the local micromechanisms of material separation along the fracture path. Engineering „brittle" fractures can occur only if the part contains a stress-concentrator, which allows local plastic deformation and fracture processes to take place at low applied stresses. The stress-concentrator may assume the form of a hole or blunt notch, or may be crack-like in nature, with a sharp tip.

Fracture processes of interest are therefore those which operate ahead of stress-concentrators in response to the high local stresses or strains. Local plastic deformation induces a high hydrostatic component of stress ahead of the tip of the stress-concentrator and this in turn is associated with values of maximum tensile stress substantially higher than the uniaxial yield stress.

In general, it is convenient to divide low-temperature fracture processes into two classes; *cracking*, which responds to tensile stress, and *rupture*, which responds to plastic strain. Micro-cracks must, however, be initiated by plastic strain and the local rupture process is often sensitive to the hydrostatic component of stress, so that it is more appropriate to refer to stress-or strain-dominance rather than to stress- or strain-control. Behaviour is strongly affected by features of microstructure; notably second-phase particles, inclusions, grain-boundaries, and the material's grain size.

To illustrate some of these microstructural features, the present paper describes three types of fracture process:

a) cleavage microcracking, initiated in brittle second-phase particles in ferritic steels at low temperatures,
b) fibrous rupture, induced by the formation of micro-voids around inclusions or other second- phase particles in structural steels and aluminium alloys,
c) high-temperature crack growth, in quenched and tempered steels, in circumstances where the rate of growth is controlled by the diffusion of sulphur to the region of high hydrostatic stress.

Cleavage Microcracking

Two main types of microstructure will be treated:

a) that of a wrought mild steel or C/Mn structural steel which has been normalised or annealed. This contains more-or-less uniform ferrite grains, of diameter in the range 10 – 100 μm with carbide present as grain-boundary films or in patches of pearlite. The inclusions present depend on deoxidation practice : rimming or semi-killed steels contain manganese silicates and manganese sulphide (MnS); fully-killed steel may also contain alumino-silicates or aluminium oxide. The carbon content of such steels is likely to be in the range 0.1 – 0.15 %.
b) that of a C/Mn weld deposit, produced, for example, by manual-metal-arc (MMA) or submerged arc(SA) welding processes. For many rates of cooling, the microstructure is likely to consist of moderately large (10 μm wide) regions of „grain-boundary" ferrite, surrounding heterogeneously nucleated intra-granular „acicular" ferrite needles of width approx. 1 μm. The boundaries between the needles are high-angle and contain martensite, retained austenite, or carbide (MAC products). Aligned MAC products may be observed in ferrite nucleated from the prior austenite grain boundaries. The carbon content of a weld metal is usually lower than that of wrought material and the volume fraction of deoxidation products (alumino-silicates, alumina) is much higher. One effect of this higher volume fraction is to provide heterogeneous nucleation sites for the acicular ferrite.

The second-phase particles play an important role in the nucleation of cleavage microcracks. Early models of cleavage in wrought mild steel envisaged the piling-up of dislocations at grain boundaries until sufficient local stress and displacement had been generated at the end of the pile-up to initiate a crack. Rigorous mathematical analyses of this model later revealed that the energetics involved with the propagation of such a nucleus implied *either* that the crack would not nucleate, *or* that it would nucleate *and* propagate catastrophically. In other words, the propagation was controlled totally by the dislocation pile-up stresses and hence only by the deviatoric component of the applied stress system [1].This conclusion was contrary to the observed influence of the maximum tensile stress in a yielded region as manifested by the effects of notches on cleavage fracture. The anomaly could be resolved if the effective work of fracture, γ_e, were to rise as the microcrack nucleus increased in size [2].This situation can be given an physical basis if the nucleus forms in a brittle second-phase particle (low γ_e) and then has to break out into the ferrite matrix (higher γ_e). Arrested micro-cracks have been observed in grain-boundary carbides in wrought steels and there is good evidence for the formation of microcracks in brittle inclusions in weld metals (see below). A number of observations of microcracks arrested at grain boundaries have also been made, but there is no direct evidence of such grain-size microcracks preceding total fracture in pre-cracked fracture toughness testpieces of low strength steels. This mechanism is more significant in lath martensitic microstructures (e. g. in 9 % Ni steel) where „packet" boundaries may provide some impedance to crack propagation.

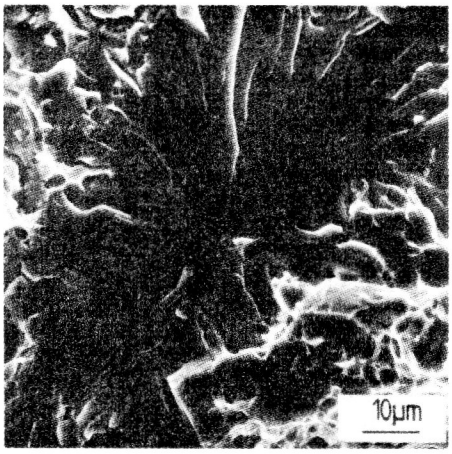

a)

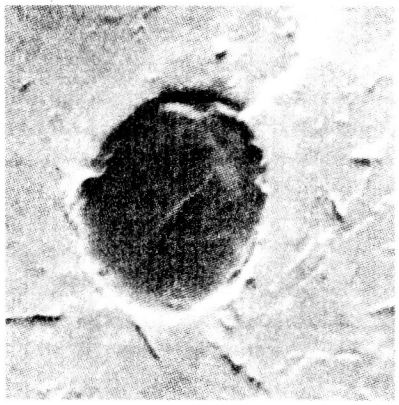

b)

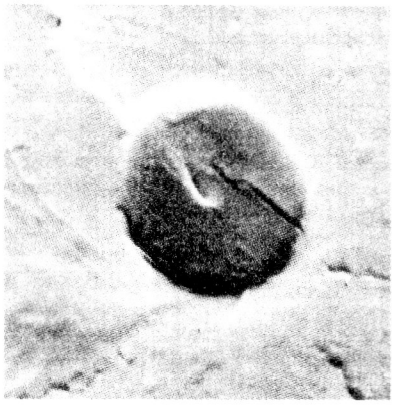

c)

Fig. 1
Fracture initiation from inclusions
a) general view of river lines diverging from an inclusion (courtesy Dr. J. H. Tweed)
b, c) two halves of a fractured inclusion from matching fracture surfaces – the maximum diameter is approx 5 μm and EDAX shows that the inclusion contains Si(courtesy Dr. M. B. D. Ellis)

Carbides have been shown to be the important microstructural feature in quenched A533B (MnMoNi) steel containing 0.25C, even though these carbides were only 30 – 40 nm thick and the steel possessed a lath martensite microstructure [3].

The quantitative modelling of microcrack propagation ahead of a notch or precrack relies on numerical analysis of the stresses in the plastic region and a knowledge of the location of the microcrack nucleus. Finite element analyses for the „small-scale" yielded crack and for one particular blunt notch-bend geometry have been available for some fifteen years and have been used to develop the theory of cleavage fracture and fracture toughness in wrought steel [4], [5], but it has not proved possible unambiguously to locate the critical carbide nucleus. It has had to be assumed in the blunt-notched test that the *maximum* value of tensile stress was that corresponding to the propagation of one of the larger carbides e. g. the 95th percentile thickness or radius. If the carbide density is sufficient, there is a high probability of finding such a carbide in the region of maximum stress. The value of this maximum stress could then be used to predict the fracture toughness of a precracked testpiece, assuming a „critical distance" (location of „potent" microcrack nucleus), which was taken to be independent of temperature, since it related to the steels microstructure [4]. The critical distance is strictly not identifiable in any deterministic way with a microstructural parameter, such as grain size, but results from a probabilistic analysis [5].

The great advantage of studying cleavage fracture in weld metals is that it is possible in some cases to locate the active microcrack nucleus [6]. Examples are shown in Fig. 1. From such observations, it is possible to identify both halves of the fractured inclusion on the matching fracture surfaces, to analyse it chemically, to determine its size and to locate its position. Using the finite element stress analysis it is then possible to calculate the stress, σ_F, *at* the site from which the microcrack propagated. Some values for σ_F determined in this way are given in Table I, [7].

From these values, it is possible to comment on two points. First, it is possible to show that σ_F varies in a linear fashion with the inverse square root of inclusion diameter, giving results similar to those (for σ_{max}) for spheroidal carbides. The failure process corresponds to a local Griffith criterion, with a value of γ_e of approx. 9 Jm^{-2}. Reasons for this value have been discussed elsewhere [8] but it is clear that γ_e must be greater than the surface energy to satisfy the tensile stress – controlled growth criterion. Table I also shows the temperature dependence of σ_F. The individual values correspond to different inclusion sizes, but within these limits, σ_F is independent of temperature.

It is also possibly to locate initiation sites in precracked testpieces although very few data are as yet available. These are presented in Table 2 together with the results of calculations of the corresponding critical distances, using the RKR model (4) obtained from the known value of fracture toughness and a value of σ_F inferred from the inclusion size and the relationship between σ_F and $(\text{diameter})^{-1/2}$. These results indicate that the assumption of a constant critical distance, independent of temperature, fits the theory but does not agree with observations, except for the highest temperatures in the range. The differences cannot be attributed to changes in

Table 1
Inclusion-initiated Cleavage in C/Mn Weld Metals
(after D. E. McRobie)

Specimen	Test Temperature °C	Inclusion Diameter μm	σ_F MPa
–	–	–	–
A	−160	1.2	2206
B	−170	4.3	1620
C	−170	2.5	1936
D	−170	0.8	1872
E	−180	1.8	2045
F	−170	0.9	1936
G	−170	1.0	1936
H	−110	1.0	1867
I	−110	0.6	1908
J	−180	0.7	2001
K	−120	0.8	1995
L	−130	1.6	2186
M	−130	1.4	2141
N	−135	2.6	1466
O	−153	1.2	1534
P	−165	1.0	1406
Q	−196	1.9	1380
R	−175	1.3	1445
S	−154	2.2	1231

A-M single pass (some strain-aged) manual metal arc
N-R two-pass submerged arc
S multipass submerged arc

Table 2
Fracture Toughness and Critical Distance, Xo
(after D. E. McRobie)

Specimen	Temperature °C	K_{IC} MPam$^{1/2}$	Xo (obs) μm	Xo (RKR) μm
T	−173	44	34	188
U	−150	49	56	220
V	−120	55	57	217
W	−100	63	190	204

T-W two-pass submerged arc

the distribution of crack nuclei, since the value of σ_F has been deduced from the fracture of a large inclusion. One possibility is that the fatigue precracking procedure at room temperature has produced a „warm prestressing" effect which assumes more importance at the lower testing temperatures.

The ability to locate microcrack nuclei represents an exciting development in the understanding of cleavage fracture criteria.

Fibrous Rupture

Structural engineering alloys are not commonly employed in situations where they are likely to fail by cleavage. Steels are used above their transition temperature, aluminium alloys are not susceptible to cleavage. Nevertheless, the highest strength steels and high strength aluminium alloys may exhibit fracture toughnesses which are only some 30 – 40 MPam$^{1/2}$, i. e. comparable with that for cleavage fracture in mild steel at low temperature.

The process of fibrous rupture in alloys involves the formation of voids around second-phase particles followed by the linkage of these voids by concentrated plastic deformation of the material between them. The simplest model is typical of fibrous rupture in a free-cutting mild steel which contains a high volume fraction of closely spaced manganese sulphide (MnS) inclusions. The thermal expansion coefficient of MnS is greater than that of the steel matrix, so that, on cooling from the hot-working temperature, the particle tries to shrink relative to the size of cavity that it occupied at high temperature. This creates tensile stress in the particle and may even give rise to debonding of the particle before any external stress is applied. The consequence is that the strain required for void initiation is virtually zero. In a precracked testpiece, the crack blunts and opens until the blunting tip coalesces with a void expanding in the region of high hydrostatic stress ahead of the tip (see Fig. 2). The value of crack tip opening desplacement (CTOD) at this point is referred to as the (fracture) initiation CTOD, δ_i. It is clear that δ_i is a function of inclusion spacing, Xo, and inclusion radius, Ro and Fig. 3 shows a plot of δ_i/Xo vs. Xo/Ro as predicted for this ideal coalescence process, [9] together with some experimental data for soft steels which follow the predictions fairly well [10]. The conclusion is that the curve in Fig. 3 represents an upper bound to δ_i, given values of Xo and Ro, which characterise the material. Since the assumptions on material deformation are perfect plasticity or power-law hardening, however, higher values may be obtained for TRIP steels, where the hardening exponent increases with strain above a critical value.

More usually, however, engineering alloys, in particular, high-strength steels and aluminium alloys. fail to exhibit

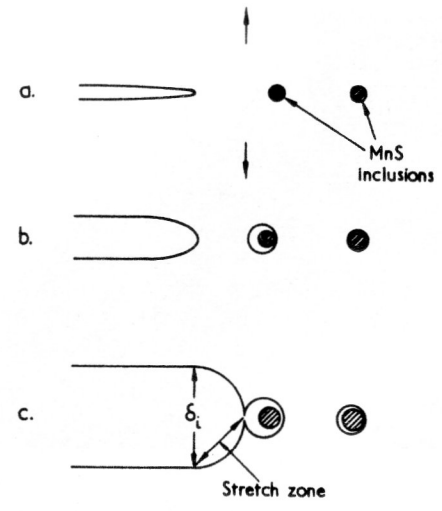

Fig. 2
Initiation of fibrous fracture

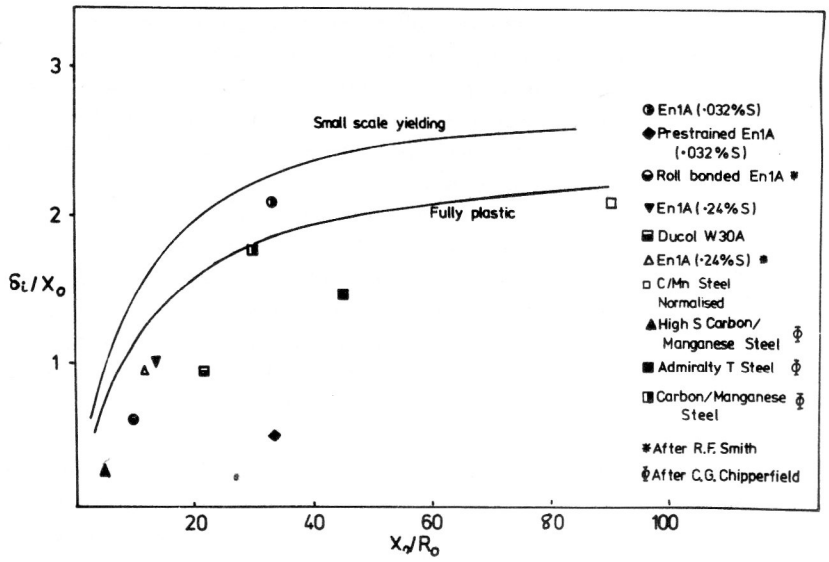

Fig. 3
Variation of CTOD with inclusion spacing and radius

„upper bound" crack-tip ductility (see Fig. 3), but suffer fibrous extension at δ_i values very much less than those predicted from the spacings of the non-metallic inclusions. The reason for this can be understood by considering the behaviour of a high-strength, quenched-and-tempered, low-alloy steel. To ensure good quality material, care is taken in steelmaking to reduce the inclusion content, so that inclusion spacings are large. Then as the region ahead of the crack tip is strained plastically in an attempt to cause the tip to coalesce with an expanding void (as in Fig. 2) it becomes possible for the dislocations created so to stress the tempered carbides that their interfaces decohere and the necking matrix is rather suddenly filled with closely spaced microvoids which link rapidly to produce „shear decohesion" which is exhibited as an incremental crack advance, see Fig. 4. This can be so discontinuous that it is recorded as a discrete event by acoustic emission equipment.
The critical strain required to initiate microvoids in a tempered steel is of order unity if the carbides are spheroidal and posses a clean carbide/ferrite interface [11].

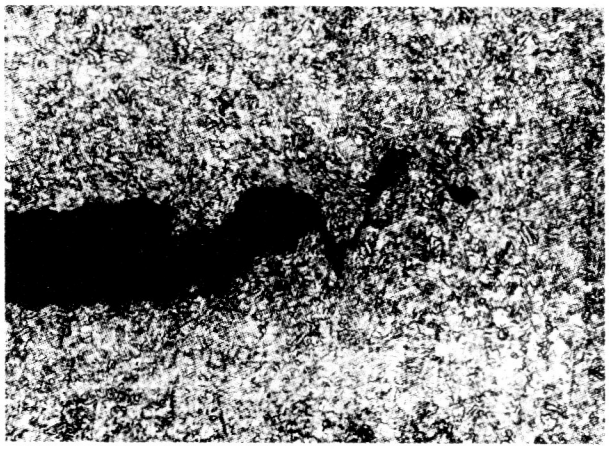

Fig. 4
Linkage of voids ahead of crack tip by „shear decohesion" (courtesy Dr. C. P. You)

For lath-like carbides, as produced by low tempering temperatures, or for interfaces weakened by impurity segregation, the initiation strains are much reduced and this is reflected by lower values of δ_i. In aluminium alloys the particles which initiate microvoids are primarily the dispersoids (in the size range 0.05 – 0.5 μm)

Fig. 5
Localisation of flow in underaged aluminium alloy (courtesy Dr. J. J. Lewandowski)

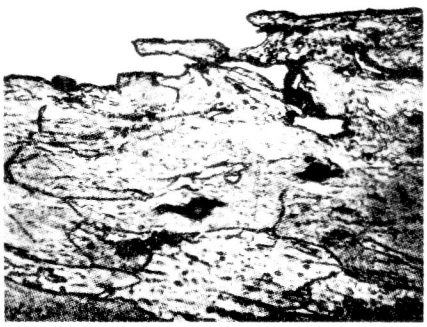

Fig. 6
Torsional failure in mild steel: the shear acts in the horizontal direction

and differences in values of δ_i have been demonstrated [12] for 7000 series (Al–Zn–Mg–Cu) alloys when the chemical nature of the dispersoids was changed by employing Zr treatment ($ZrAl_3$) rather than Cr-treatment (E-phase). The state of aging of the alloy is also of importance and Fig. 5 shows the degree of localisation of flow that can occur at the root of a notch for a severely under-aged aluminium alloy, whose strain-hardening rate is very low [13]. Similar effects are observed for heavily cold-worked low-strength steels and, by implication, for material subjected to heavy neutron irradiation. These final modes of separation seem to be more connected with a genuine „shear decohesion" of the matrix, in which inclusions or second-phase particles play a secondary, rather than a primary role. The situation is perhaps analogous to that of torsional failure in mild steel, as illustrated in Fig. 6.

High Temperature Crack Growth

If a low-alloy steel containing sulphur is rapidly quenched from a high austenitising temperature (ca. 1250 °C), the sulphur is largely retained in super-saturated solid solution. If the cooling-rate from 1250 °C is slower (although still sufficient to give a martensitic structure) the sulphur is effectively all precipitated at the prior austenite grain-boundaries as MnS particles. When the steel is subsequently stressed at temperatures in the range 450 – 650 °C (as may occur, for example, during part of the stress-relieving heat-treatment given to the heat-affected-zone around a weld), its behaviour is critically dependent on the amount of „free" sulphur (i. e. the amount not „fixed" as MnS). If most of the sulphur is free, it is possible to obtain a form of brittle intergranular fracture – low ductility intergranular fracture (LDIGF) which exhibits rather „clean", smooth facets – see Fig. 7 and Ref. 14. This mode is observed at lower temperatures in the range. If the sulphur is fixed, LDIGF is not observed, but low strain intergranular fracture can still be obtained at higher temperatures in the range, the facets are, however, now covered with fine-scale dimples centred on the MnS particles located at the prior austenite grain boundaries. This mode is referred to as intergranular micro-void coalescence – IGMVC.

An intriguing fact is that, if the LDIGH crack is grown partially through a test piece, and the testpiece is then unloaded and fractured at – 196 °C, the subsequent low temperature fracture does not continue to follow the intergranular path, but changes to transgranular cleavage, Fig. 8. There has, therefore, been no general embrittlement of the boundaries at high temperature, and it was deduced that the reason for the grain – boundary separation was that free sulphur diffused to grain boundaries in the region of high hydrostatic stress ahead of the crack tip, reducing grain boundary cohesion [14], [15]. The effect may be observed in blunt-notched testpieces, Fig. 9, and the rates of crack growth at different temperatures may be analysed to derive an activation energy which is comparable with that for the diffusion of sulphur in iron [16], [17]. The process is similar to that associated with some forms of hydrogen cracking in steels at ambient temperatures. Models for the drift of sulphur atoms involve the stress field of the crack and grain-boundary sinks [18].

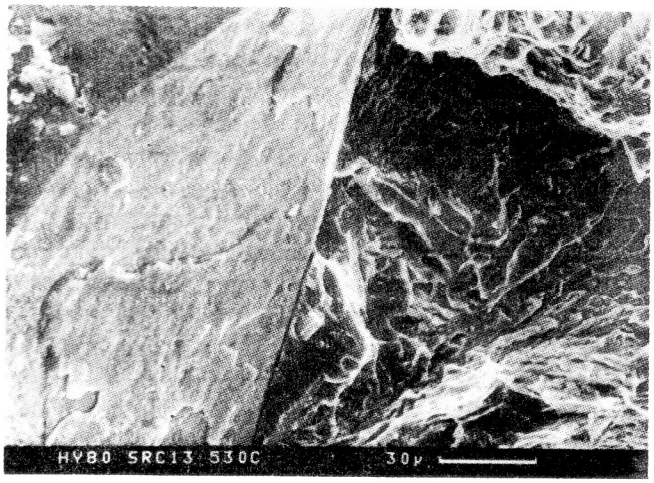

Fig. 8
Interface between LDIGF facet (left at 530 °C and transgranular cleavage facet (right) produced on subsequent fracturing at – 196 °C (courtesy Dr. C. P. You)

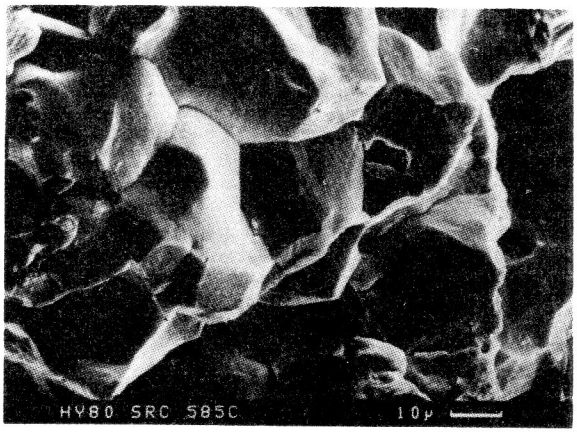

Fig. 7
Example of LDIGF (courtesy Dr. C. P. You)

Fig. 9
Formation of LDIGF *below* notch root (after Ref. 16)

The monotonic crack growth bears some similarities to creep-crack propagation, although it occurs in much shorter time-scales; it provides a very good system for exploring effects of frequency on cyclic crack growth at temperatures around 500 °C. Some success has been obtained with a simple analysis, which calculates the increments of „monotonic" growth, superimposed on the baseline „cyclic" growth, as a result of the different times spent at each of the maximum stress intensity values associated with a particular wave-form [19]. For a 2.25 CrlMo steel at 500 °C, effects of reducing frequency from 60 Hz to 0.1 Hz were well predicted: over this range, the growth-rate was observed to increase by some two orders of magnitude. Eventually, work of this sort, combined with a knowledge of activation energies, should enable crack growth rates to be expressed as functions of stress-intensity, temperature, frequency and wave-shape. There is some evidence that similar effects may occur in non-ferrous alloys, e. g. lead diffusion in aluminium alloys.

Conclusions

The paper has described the features of „classical" cracking and rupture modes of fracture and has introduced an intriguing new set of observations on high-temperature crack growth. In the introduction, it was pointed out that fractures in general are stress-dominated or strain-dominated. This may be apparent from behaviour in the simple notched-bar or fracture toughness tests described in the paper. but a critical additional piece of evidence may be obtained by testing specimen in mixed mode I (opening)/ mode II (shearing) stress systems. This is done conveniently by using symmetrical or antisymmetrical edge-cracked bend bars [20]. For a tensile stress-dominated fracture, the crack path rotates with increasing mode II so as to run normal to the maximum tangential stress in the specimen. For strain-dominated fracture, the increased shear simply causes the crack faces to slide past each other. These differences may be observed in steel specimens broken below and above the cleavage/rupture transition temperature and the testing method therefore holds great promise for in investigating the dominant factor in a new, unexplored fracture process, such as that of high temperature crack growth.

Acknowledgements

The author wishes to thank Prof. D. Hull F. Eng. for provision of research facilities.

REFERENCES

[1] Smith, E. and Barnby, J. T.: Met. Sci. Jnl. 1967, *1*, p. 56.
[2] Smith, E.: Proc. Conf. Physical Basis of Yield and Fracture. Inst. Physics and Physical Soc. Oxford. 1966, p. 36.
[3] Bowen, P., Druce, S. G. and Knott, J. F.: Acta Met., 1987, *35*, p. 1735.
[4] Ritchie, R. O., Knott, J. F. and Rice, J. R.: Jnl. Mech. Phys. Solids. 1973, *21*, p. 395.
[5] Curry, D. A. and Knott, J. F.: Met. Sci., 1979, *13*, p. 324.
[6] Tweed, J. H. and Knott, J. F.: Acta. Met., 1987, *35*, p. 1401.
[7] McRobie, D. E.: „Cleavage Fracture in C-Mn Weld Metals" PhD Thesis, Univ. of Cambridge, May 1985.
[8] Knott, J. F.: „Yield, Flow and Fracture of Polycrystals" ed. T. N. Baker, Applied Science, 1983, p. 81.
[9] Rice, J. R. and Johnson, M. A.: „Inelastic Behaviour of Solids" ed. M. F. Kanninen et al, McGraw Hill, 1970, p. 641.
[10] Green, G. and Knott, J. F.: Jnl. Eng. Matls. and Tech., ASME H, 1976, *98*, p. 37.
[11] Knott, J. F.: Met. Sci. 1980, *14*, p. 327.
[12] Chen, C. Q. and Knott J. F.: Met. Sci. 1981, *15*, p. 357.
[13] Lewandowski, J. J. and Knott, J. F.: Proc. 7th Intl. Conf. on Strength of Metals and Alloys, Montreal 1985, ed. McQueen et al, Pergamon, p. 1193.
[14] You, C. P., Hippsley, C. A. and Knott, J. F.: Met. Sci. 1984, *18*, p. 387.
[15] Bowen, P. Hippsley, C. A. and Knott, J. F.: Acta. Met. 1984, *32*, p. 637.
[16] Lewandowski, J. J., Hippsley C. A., Ellis, M. B. D. and Knott, J. F.: Acta. Met. 1987, *35*, p. 593.
[17] Lewandowski, J. J., Hippsley, C. A. and Knott, J. F.: Acta. Met. 1987, *35*, p. 2081.
[18] Streitenberger, P. and Knott, J. F.: Scripta Met. 1987, *21*, p. 1363.
[19] Bowen, P., Hippsley, C. A. and Knott, J. F.: Proc. 6th Europ. Conf. on Fracture., EMAS, 1986, p. 1927.
[20] Maccagno, T. M. and Knott, J. F.: ibid. p. 1453.

Name of the author:

Dr. J. F. Knott
Department of Materials Science and Metallurgy
University of Cambridge
Cambridge CB2 3QZ
England